HEPATOBILIARY

CrossMark

Magnetic resonance elastography SE-EPI vs GRE sequences at 3T in a pediatric population with liver disease

Juan S. Calle-Toro[1] · Suraj D. Serai[1,4] · Erum A. Hartung[2,4] · David J. Goldberg[3,4] · Bradley D. Bolster Jr.[5] · Kassa Darge[1,4] · Sudha A. Anupindi[1,4]

Abstract

Purpose The goal of our study is to compare hepatic stiffness measures using gradient-recalled echo (GRE) versus spin-echo echo planar imaging (SE-EPI)-based MR Elastography (MRE) at 3T used to measure hepatic stiffness in a patients with suspected liver diseases.

Materials and methods This retrospective study included 52 patients with liver disease who underwent a 3T MRE exam including both an investigational SE-EPI-based technique and a product GRE-based technique. Regions of interest (ROI) were placed on the elastograms to measure elastography-derived liver stiffness as well as the area included within the ROIs. The mean liver stiffness values and area of ROIs were compared.

Results The mean liver stiffness was 3.72 kilopascal (kPa) ± 1.29 using GRE MRE and 3.78 kPa ± 1.13 using SE-EPI MRE. Measurement of liver stiffness showed excellent agreement between the two pulse sequences with a mean bias of − 0.1 kPa (range − 1.8 to 1.7 kPa) between sequences. The mean measurable ROI area was higher with SE-EPI (313.8 cm^2 ± 213.8) than with the GRE technique (208.6 cm^2 ± 114.8), and the difference was statistically significant ($P < 0.05$).

Conclusions Our data shows excellent agreement of measured liver stiffness between GRE and SE-EPI-based sequences at 3T. Our results show the advantage of a SE-EPI MRE sequence in terms of image quality, ROI size and acquisition time with equivalent liver stiffness measurements as compared to GRE-MRE sequence.

Keywords Fibrosis · Liver · Magnetic resonance imaging · MR elastography · GRE MRE · SE-EPI MRE

Juan S. Calle-Toro and Suraj D. Serai have contributed equally to this work.

✉ Suraj D. Serai
serais@email.chop.edu

1 Division of Body Imaging, Department of Radiology, Children's Hospital of Philadelphia, 3401 Civic Center Blvd, Philadelphia, PA, USA

2 Division of Nephrology, Department of Pediatrics, Children's Hospital of Philadelphia, Philadelphia, PA, USA

3 Division of Cardiology, Department of Pediatrics, Children's Hospital of Philadelphia, Philadelphia, PA, USA

4 Perelman School of Medicine, University of Pennsylvania, Philadelphia, PA, USA

5 Siemens Healthineers, Malvern, PA, USA

Introduction

Liver diseases remain a common cause of morbidity and mortality among adults and children across the globe [1]. In the United States, an increase in prevalence of fatty liver disease among children has been associated with an overall increase in liver disease [2]. Chronic liver conditions can lead to liver fibrosis. At our institute, liver fibrosis has been observed in patients with congenital heart disease, especially in patients with Fontan palliation and in patients with autosomal-recessive polycystic kidney disease (ARPKD) [3–5]. Liver fibrosis is multifactorial and early diagnosis and staging are important factors contributing to a better outcome [6]. Liver biopsy is unsuitable as a routine follow-up assessment [6–14]. Studies have reported the risk of hospitalization related to a liver biopsy in the range from 1% to 5%, with an additional 0.57% risk of severe complications, and reported mortality rates ranging from 1:1000 to 1:10000 [15–19]. Magnetic resonance imaging (MRI)

has higher acceptance to diagnose liver fibrosis, with the advantage of being non-invasive [6]. Liver fibrosis results from collagen deposition which increases the organ's stiffness [20]. Magnetic resonance elastography (MRE) is an imaging technique that indirectly assesses the mechanical properties and can measure tissue stiffness [21–23]. The two types of acquisition sequences currently in use to obtain liver stiffness values are the gradient-recalled-echo (GRE) based and the spin echo (SE) based with echo-planar read out; both of which have been shown to have excellent correlation [24].

The use of GRE-based sequence has demonstrated to correlate with histological grading of liver fibrosis in previous studies and a recent meta-analysis [25–28]. However, the inherent limitations of GRE-based acquisition on 3T in addition to enhanced sensitivity to susceptibility, is the signal drop off due to longer echo time (TE) and relatively shorter T2 relaxation time of the liver. GRE based MRE also has relatively lower accuracy in obese patients due to the increased distance from the driver to the liver. Thicker layers of fat can result in signal loss and produce limitations for encoding shear waves in the deeper areas of the liver, hence reducing the resulting stiffness measurable area [24]. Since chronic liver disease is quite frequently associated with obesity, radiologists should be aware of the limitations of GRE-based acquisition in such cases. GRE-based MRE acquisition also require relatively longer periods of acquisition and have higher susceptibility to breathing motion. The current GRE-based protocol, for MRE image acquisition requires, a breath hold of approximately 20 seconds for a single slice [21, 29] (Fig. 1a). Echo-planar imaging (EPI), on the other hand, is a fast magnetic resonance imaging technique that obtains all spatial-encoding information in a single radiofrequency (RF) pulse, allowing faster acquisition times with less motion artifacts [30]. SE-EPI-based images are advantageous in pediatric patients because they allow for image acquisition of multiple slices within only one breath hold, and also enable measuring larger areas of the liver due to higher waves encoded per relaxation time (TR) [21, 23, 30–32] (Fig. 1b).

The aim of our study was to compare GRE versus SE-EPI-based sequences in MRE at 3T used to measure hepatic stiffness in patients with suspected liver disease.

Methods

This was an institutional review board (IRB) approved and Health Insurance Portability and Accountability Act (HIPAA) compliant study. We included an investigational 2D SE-EPI MRE sequence in a consecutive series of pediatric patients who underwent 2D GRE MRE for clinical indications or who were part of existing IRB-approved research protocols between October 2014 and July 2018.

Informed consent was obtained for the investigational SE-EPI MRE acquisition. Patients with non-diagnostic studies were excluded.

MRE set up

After consent from both research and referred clinical subjects, MRE of the liver was performed on a 3T MR scanner (MAGNETOM Skyra, Siemens Healthineers, Malvern, PA, USA) equipped with a pediatric mechanical driver positioned over the right upper quadrant of the liver coupled with a commercially available active MRE driver (Resoundant, Rochester, MN) via a length of plastic tubing (Fig. 2a). The mechanical excitation frequency was 60 Hz and was synchronized to the MRE pulse sequence [21]. The initiation and cessation of the vibrations are controlled by the MR pulse sequence programmed and embedded as part of the scanner software. The MRE pulse sequence did not bypass any scanner safety standards as specified by the manufacturer.

Image acquisition

For the MRE sequences, four contiguous axial slices through the broadest section of the liver were prescribed from the coronal localizer images (Fig. 2b). For the GRE sequence, four contiguous slices were acquired sequentially at 1 breath-hold (BH) per slice for a total of 4 BHs. The SE-EPI sequence acquired all four different slices in a single BH. MRE protocol parameters of 2D GRE and 2D SE-EPI sequences are outlined in Table 1. The frequency of applied vibrations was kept identical for both pulse sequences at 60 Hz. Geometry parameters, such as field of view, section thickness, and number of sections, were kept identical on both sequences. The MRE acquisitions were performed back to back, with ordering of the sequences determined by the MR technologist; no effort was made to control the order of acquisitions. For this study, we focused on a comparison between the sequences without correlation with clinical data or liver histopathology. Increased (abnormal) stiffness was defined as values > 2.9 kPa [22, 23, 29].

Image processing

Both 2D GRE and 2D SE-EPI MRE sequences generated elastograms for each acquired slice automatically on the scanner. MRE maps and pulse sequence were generated for each patient using a multimodal direct inversion algorithm (Mayo Clinic, Rochester, MN, USA) with regions of interest (ROIs) independently drawn on each image. 95% confidence
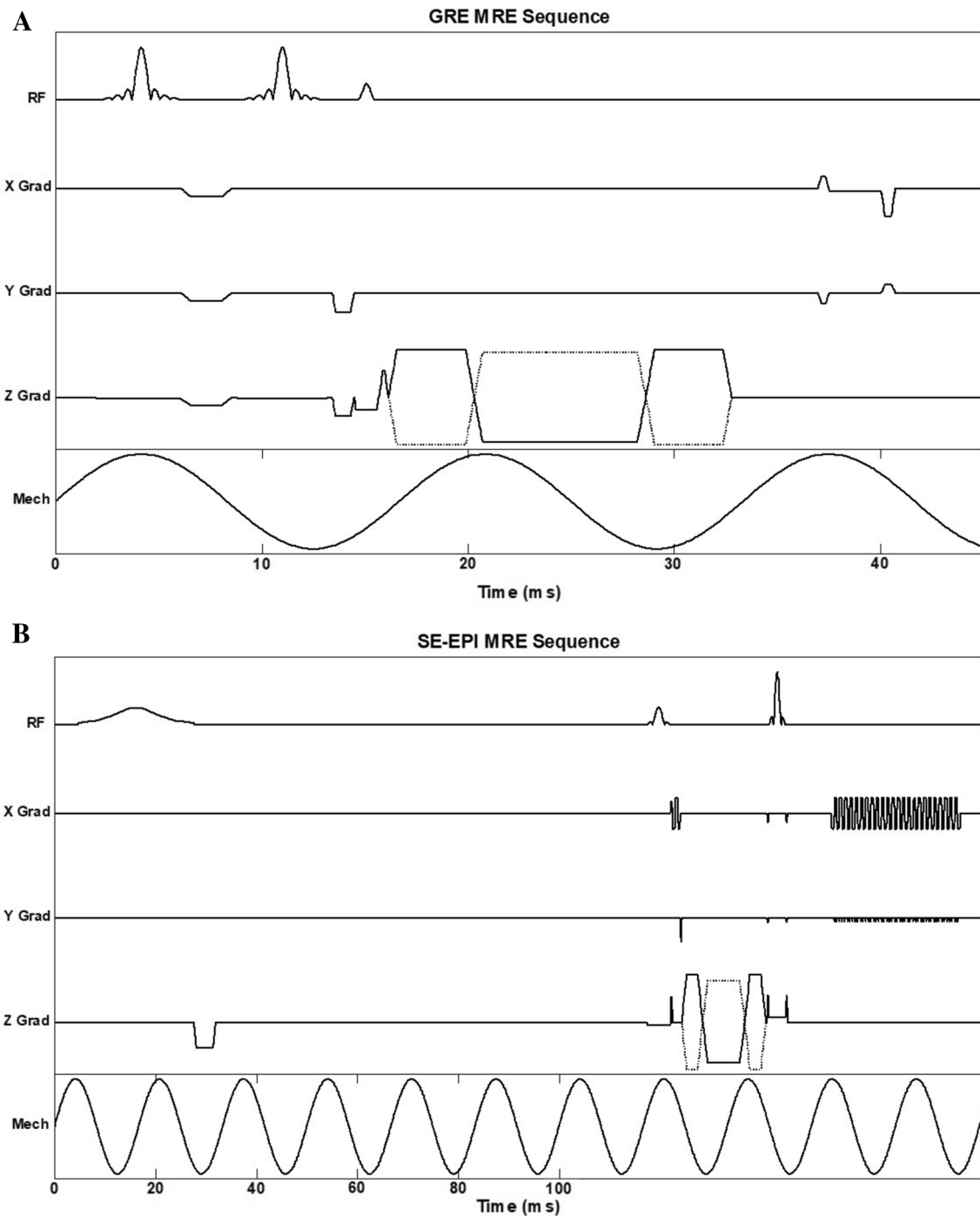
Fig. 1 a GRE and **b** SE-EPI acquisition sequence timing diagram. *RF* radiofrequency, *Grad* gradient, *ms* milliseconds, *Mech* mechanical excitation

maps were automatically generated and overlaid on the MR elastograms during post-processing. These maps are indicative of the quality of the wave data and appear as a checkerboard pattern overlay in areas of low-quality data.

Image artifact review

All MRE images were reviewed qualitatively on both sets of images for any breathing or motion artifacts that rendered the images undiagnostic.

Fig. 2 a MRE positioning and **b** slice locations
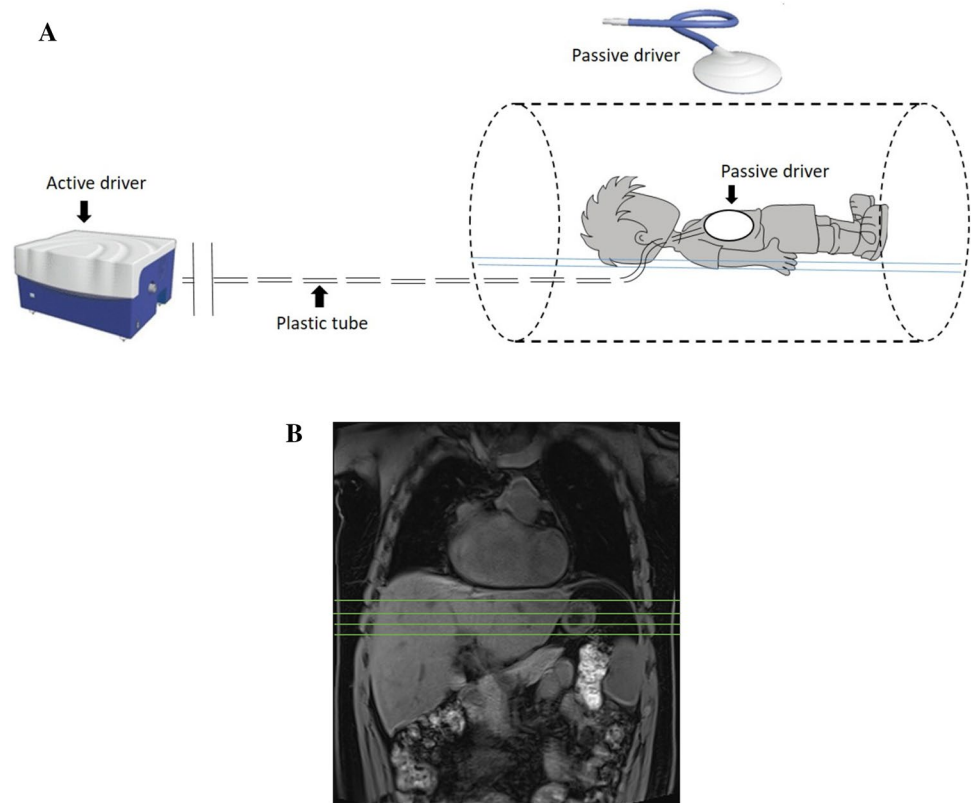
Table 1 MRE protocol parameters at 3T (scanner model used: Siemens Skyra)

Parameter	2D GRE MRE	2D SE-EPI MRE
TR (msec)	50	1000
TE (msec)	23.7	30
Matrix size	128 × 64 interpolated to 128 × 128	100 × 100 (true)
Voxel size (mm)	1.2 × 1.2	1.5 × 1.5
Slice thickness (mm)	6	6
Bandwidth (Hz/Px)	399	2380
No. of averages	1	1
No. of slices	4	4
MEG frequency (Hz)	60	60
MEG direction	Z axis (slice)	Z axis (slice)
Echo spacing (msec)	24.7	0.5
EPI factor	NA	100
Acceleration factor	2	2
Scan time (min:sec)	1:00	0:11

GRE gradient recalled echo, *SE-EPI* spin echo-echo planar imaging, *2D* two dimensional, *MRE* magnetic resonance elastography, *MEG* motion encoding gradients, *msec* milliseconds, *mm* millimeters, *Hz* hertz, *mT/m* millitesla/meter, *Px* pixel, *min* minutes; *sec* seconds, *NA* not applicable

Image analysis

ROIs were drawn in random order on the elastograms, magnitude image and confidence maps by a single observer blinded to the method of acquisition; and liver stiffness was measured in kilopascals (kPa). ROIs for measurement of liver stiffness were drawn within the regions bound by the confidence maps in a manner to include as much of the liver parenchyma as possible while staying approximately 2 mm within the outer liver capsule and excluding large vessels and the central biliary tree. The elastograms included a superimposed confidence mask representing the areas where the inversion algorithm deemed the measured mechanical waves of insufficient quality. ROIs were drawn on the elastograms avoiding areas with the confidence mask. The corresponding magnitude image and wave images were used as a guide. For statistical comparisons, liver stiffness was expressed as a mean of mean stiffness values measured on each section (in kilopascals, kPa). ROI size (in square centimeters) was recorded for each section for each patient at each pulse sequence, and comparison was made between summated ROI sizes (i.e., the sum of ROI size across all sections in a given patient). For each sequence and each slice the mean stiffness was calculated. Overall liver stiffness was calculated as the average of stiffness values from each slice, weighted by the ROI area of each slice.

Statistical analysis

Mean liver stiffness and summated ROI sizes for each patient were compared between 2D GRE and 2D SE-EPI MRE images using paired *t* tests (two tailed) and Pearson's correlation. Correlation coefficients were classified using the following definitions: 0–0.19, very weak; 0.2–0.39, weak; 0.40–0.59, moderate; 0.60–0.79, strong; and 0.80–1.0, very strong [33]. Our hypothesis is that there is no significant difference in measured stiffness values between the two acquisition methods. Null hypothesis can be rejected if there is a statistically significant difference between the two groups.

Scatter plots and Bland-Altman plots were generated to assess agreement and bias between 2D GRE MRE and 2D SE-EPI MRE-derived liver stiffness values. A *P* value < 0.05 was considered statistically significant for all inference testing and 95% confidence intervals were calculated, where appropriate. Statistical analyses were performed using statistical software (MedCalc Statistical Software version 15.8, MedCalc, Ostend, Belgium; and SAS version 9.3, SAS Institute, Cary, NC).

Results

Patients

The study included 52 patients (17 females, 35 males). All subjects were imaged using both the 2D GRE and 2D SE-EPI sequences. There were no technical issues that precluded the acquisition of either sequence during this study. Mean age of the population with both scans was 17.6 years ± 4.7 (range 9.1 to 35.6 years; 6 patients with Fontan had age > 21 years).

Indications for the MRE examinations included: 39 studies with prior Fontan operation (75.0%); 4 studies of patients with ARPKD (7.7%); 4 subjects with liver studies as healthy controls for a prospective ARPKD study (7.7%), 2 patients with history of elevated liver enzymes and suspected nonalcoholic fatty liver disease; 1 patient with Wilson's disease; 1 patient with chemotherapy- resistant liver metastasis from primary lymphocytic tumor; and 1 patient with referral for MRI scan to evaluate liver disease related to Tetralogy of Fallot.

2D GRE versus 2D SE-EPI liver stiffness measurement correlation and agreement

The mean liver stiffness values were 3.72 kilopascal (kPa) ± 1.29 using GRE MRE and 3.78 kPa ± 1.13 using SE-EPI MRE. Measurement of liver stiffness showed excellent agreement on both pulse sequences. A comparison of means by t test gives a difference of 0.06 kPa (95% CI
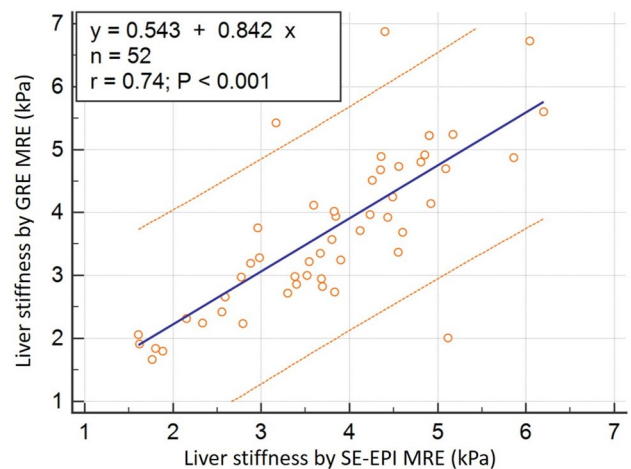

Fig. 3 GRE and SE-EPI MRE correlation. Scatter plot shows strong correlation between liver stiffness values obtained by GRE and SE-EPI MRE methods. With the exception of borderline outliers, all values fall within 95% prediction limits ($r = 0.74$; $P < 0.001$)
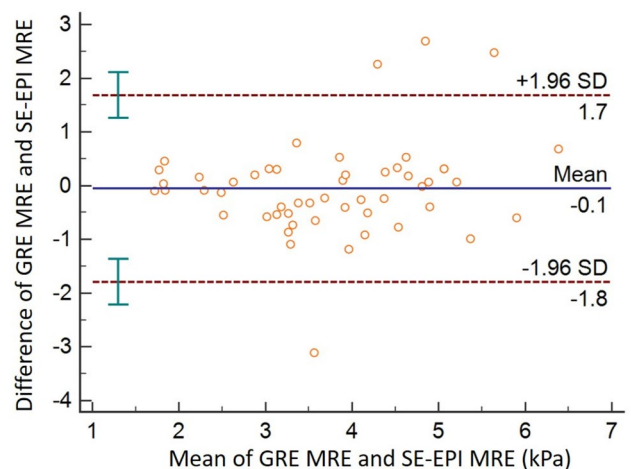

Fig. 4 Bland and Altman plot shows all studies fall within two standard deviations ($P < 0.001$)

−0.41 to 0.53) with a significance level $P = 0.8$. Correlation between liver stiffness measured on 2D GRE and 2D SE-EPI MRE sequences was strong ($r = 0.74$; $P < 0.001$). With the exception of borderline outliers all stiffness values fell within 95% prediction limits of 2D GRE versus 2D SE-EPI agreement (Fig. 3). The reason for the outliers was due to smaller regions of the liver on the GRE method as compared to larger areas of the liver on the SE-EPI method. Bland–Altman analysis demonstrated a mean bias of −0.1 kPa (range −1.8 to 1.7 kPa) between sequences (Fig. 4).

The mean area of the liver stiffness ROI was higher on SE-EPI (313.8 cm^2 ± 213.8) than on GRE (208.6 cm^2 ± 114.8), and the difference was statistically significant ($P = 0.002$) (Fig. 5). A representative image of MRE stiffness maps is
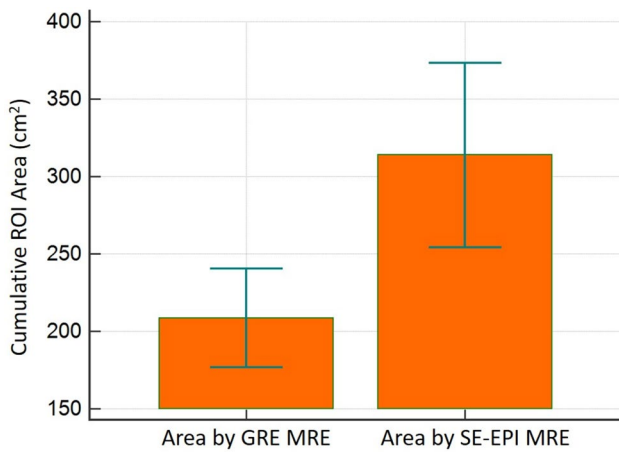
Fig. 5 Bar graphs comparing liver parenchyma areas included by regions of interest. SE-EPI MRE allowed for stiffness measurements across larger areas of the liver

shown in Fig. 6. Comparison of results between GRE and SE-EPI based MRE are summarized in Table 2. Although no scoring was given, relatively higher motion artifacts due to breathing was observed on the GRE when compared with the SE-EPI sequence (Fig. 7).

Discussion

MRE has become an important diagnostic tool for the detection and serial evaluation of liver fibrosis. This technique is more precise than ultrasound and has significant advantages relative to liver biopsy as it is non-invasive and capable of a global assessment [34]. Although, most published studies performed on pediatric patients up until now have used the traditional GRE-based MRE acquisition sequence [3, 21, 23, 35, 36], we believe there may be advantages to using the new SE-EPI-based acquisition sequence. An investigation SE-EPI-based MRE sequence was available at our institution which offered an alternative technique that was less sensitive to susceptibility-induced signal loss, more robust at 3T and offered greater patient comfort with fewer and shorter breath-holds. We found that the liver stiffness measurements using the SE-EPI-based sequence was superior to the GRE sequence in detecting liver stiffness in children with suspected liver disease in capturing larger regions of liver parenchyma, thereby further reducing sampling error. In addition, SE-EPI based sequences are advantageous as all the slices are acquired in a single breath hold, making it a much faster acquisition sequence. Qualitatively, we observed between both sequences that GRE overall presented a
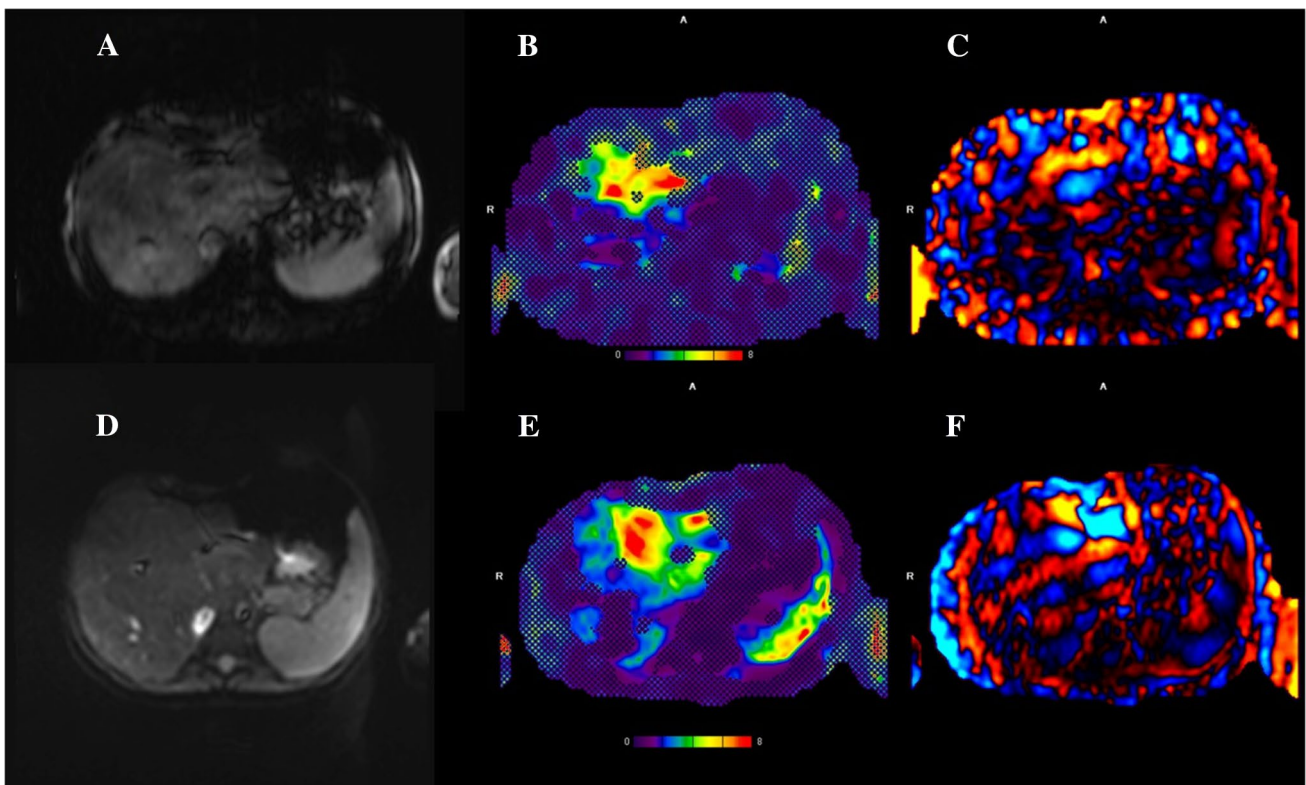

Fig. 6 Representative image of a 19-year-old female with hypoplastic right ventricle status post Fontan procedure. **a** Magnitude, **b** elastogram and **c** wave image from GRE based MRE and **d** magnitude, **e** elastogram and **f** wave image from SE-EPI based MRE

Table 2 Summary of results from GRE and SE-EPI MRE comparison

Method	GRE MRE	SE-EPI MRE
Number of patients	52	52
Mean liver stiffness (kPa)	3.72 ± 1.29	3.78 ± 1.13
Range of liver stiffness (kPa)	1.67–6.88	1.61–6.20
Mean cumulative ROI (cm^2)	208.6 ± 114.8	313.8 ± 213.8
Range of ROI (cm^2)	39.2–475.8	51.5–978.8

GRE gradient recalled echo, *SE-EPI* spin echo-echo planar imaging, *kPa* kiloPascals, *ROI* region of interest

relatively higher rate of motion artifacts due to breathing when compared with the SE-EPI sequence. A similar difference has been reported in previous studies [37], in which GRE sequence required that the patient perform sequential breath holds (four at 20 s each) to sample multiple sections of the liver [25, 28, 38–41]. This may be difficult for children to achieve without anesthesia support and could result in breathing motion artifacts and hence poor quality of stiffness maps when using the GRE method.

Image quality depends on signal and field strength, and previous studies on children were performed on 1.5T MRI machines [7, 39, 40, 42]. However, at our center, we routinely use 3T MR machines for liver imaging. On 3T, SE-EPI method has an inherent limitation of higher sensitivity to chemical shift effects. A use of fat saturation pulse can alleviate this effect. The signal acquired from using SE-EPI on 3T has increased sensitivity to susceptibility-based signal loss; whereas, the signal from the GRE-based MRE acquisition tends to decay faster due to relatively shorter liver T2 on 3T as compared to 1.5T scanner. Therefore, this technical difference could be a major factor to consider in the
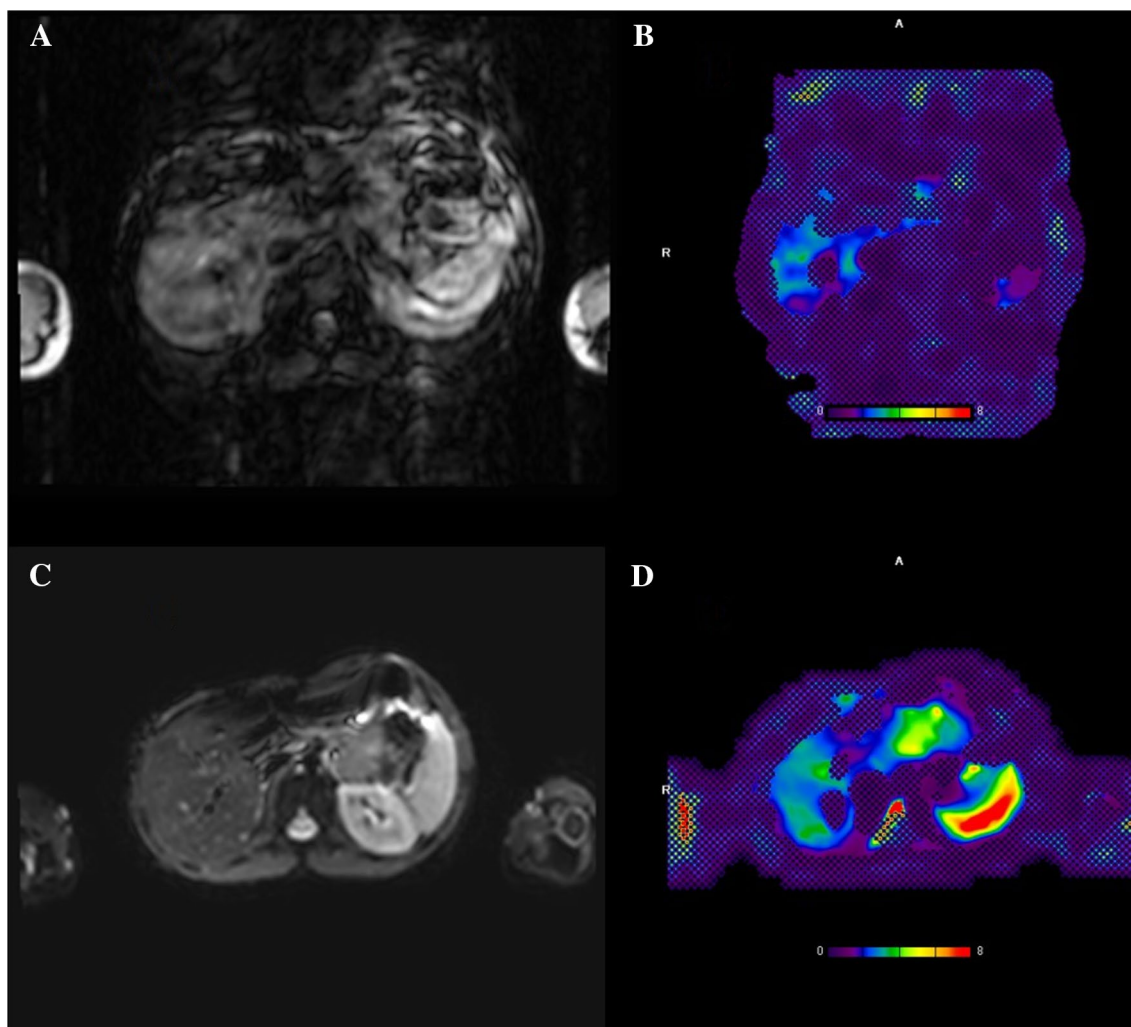

Fig. 7 Representative image of a 11-year-old female showing the importance of shorter breath hold. **a** Magnitude and **b** elastogram from GRE-based MRE versus **c** magnitude and **d** elastogram from SE-EPI-based MRE on the same patient obtained subsequently scanned back to back

evaluation of liver fibrosis. Our study, like previous studies by Felker et al. performed at 3T, has shown equally excellent agreement in stiffness values between GRE and SE-EPI sequences [43]. No pediatric patients were included in this prior study. Similar results were also seen in a study by Bae et al. on adult healthy organ donors [40]. Contrary to our findings, a relatively larger ROI was found on GRE-based MRE as compared to SE-EPI MRE. This may be due to the use of two acoustic pressure drivers placed on the patient's right and left upper abdomen adjacent to the liver and spleen. Our study, in comparison, used a single acoustic driver. In addition, the study by Bae et al. did not involve pediatric subjects.

Our study presents some limitations. In addition to the small and heterogeneous patient population, one of the limitations of our study was that we did not perform an invasive assessment of the liver for determination and quantification of fibrosis, fat and iron content as a standard of reference. However, our intent was only to compare MRE-derived stiffness values from two different acquisition methods. Second, we did not perform follow-up assessment on patients to determine whether the larger ROIs available on SE-EPI versus GRE sequence could lead to better outcomes. For this, prospective studies would be needed.

Conclusion

Our data shows excellent agreement on measured liver stiffness between 2D GRE and 2D SE-EPI sequences. Our results also show the advantage of a SE-EPI MRE sequence in terms of image quality and ROI size.

References

1. Dhole, S.D., et al., *Chronic Liver Diseases in Children: Clinical Profile and Histology.* J Clin Diagn Res, 2015. **9**(7): p. SC04-7.
2. Lobstein, T., et al., Child and adolescent obesity: part of a bigger picture. Lancet, 2015. **385**(9986), p. 2510-20
3. Wallihan, D.B., et al., *Relationship of MR elastography determined liver stiffness with cardiac function after Fontan palliation.* J Magn Reson Imaging, 2014. **40**(6), p. 1328-35
4. Serai, S.D., et al., *Magnetic resonance elastography of the liver in patients status-post fontan procedure: feasibility and preliminary results.* Congenit Heart Dis, 2014. **9**(1), p. 7-14
5. Gunay-Aygun, M., et al., *Characteristics of congenital hepatic fibrosis in a large cohort of patients with autosomal recessive polycystic kidney disease.* Gastroenterology, 2013. **144**(1), p. 112-121.e2
6. Rockey, D.C., et al., *Liver biopsy.* Hepatology, 2009. **49**(3), p. 1017-44
7. Cunha, G.M., et al., *Feasibility and agreement of stiffness measurements using gradient-echo and spin-echo MR elastography sequences in unselected patients undergoing liver MRI.* Br J Radiol, 2018. **91**(1087), p. 20180126
8. German, A.L., et al., *Can reference images improve interobserver agreement in reporting liver fibrosis?.* J Clin Pathol, 2018. **71**(4), p. 368-371
9. Jung, E.S., et al., *Interobserver Agreement on Pathologic Features of Liver Biopsy Tissue in Patients with Nonalcoholic Fatty Liver Disease.* J Pathol Transl Med, 2016. **50**(3), p. 190-6
10. Pournik, O., et al., *Inter-observer and Intra-observer Agreement in Pathological Evaluation of Non-alcoholic Fatty Liver Disease Suspected Liver Biopsies.* Hepat Mon, 2014. **14**(1), p. e15167
11. Maharaj B Fau - Maharaj, R.J., et al., *Sampling variability and its influence on the diagnostic yield of percutaneous needle biopsy of the liver.* (0140-6736 (Print)).
12. Ratziu, V., et al., *Survival, liver failure, and hepatocellular carcinoma in obesity-related cryptogenic cirrhosis.* Hepatology, 2002. **35**(0270-9139 (Print)): p. 1485-93.
13. Bedossa, P., V. Dargere D Fau - Paradis, and V. Paradis, *Sampling variability of liver fibrosis in chronic hepatitis C.* Hepatology, 2003. **38**(0270-9139 (Print)): p. 1449-57.
14. Regev, A., et al., *Sampling error and intraobserver variation in liver biopsy in patients with chronic HCV infection.* Am J Gastroenterol, 2002. **97**(0002-9270 (Print)): p. 2614-8.
15. Cadranel, J.F., F. Rufat P Fau - Degos, and F. Degos, *Practices of liver biopsy in France: results of a prospective nationwide survey. For the Group of Epidemiology of the French Association for the Study of the Liver (AFEF).* Hepatology, 2000. **32**(0270-9139 (Print)): p. 477-81.
16. Froehlich, F., et al., *Practice and complications of liver biopsy. Results of a nationwide survey in Switzerland.* Dig Dis Sci, 1993. **38**(0163-2116 (Print)): p. 1480-4.
17. Piccinino F Fau - Sagnelli, E., et al., *Complications following percutaneous liver biopsy. A multicentre retrospective study on 68,276 biopsies.* (0168-8278 (Print)).
18. Perrault J Fau - McGill, D.B., et al., *Liver biopsy: complications in 1000 inpatients and outpatients.* (0016-5085 (Print)).
19. Bravo, A.A., Sheth, S.G., Chopra, S., *Liver Biopsy.* New England Journal of Medicine, 2001. **344**(7), p. 495-500
20. Watanabe, A., et al., *Magnetic resonance imaging of the cirrhotic liver: An update.* World J Hepatol, 2015. **7**(3). p. 468-87
21. Serai, S.D., Towbin, A.J., Podberesky, D.J, *Pediatric liver MR elastography.* Dig Dis Sci, 2012. **57**(10), p. 2713-9
22. Trout, A.T., et al., *Diagnostic Performance of MR Elastography for Liver Fibrosis in Children and Young Adults with a Spectrum of Liver Diseases.* Radiology, 2018: p. 172099.
23. Xanthakos, S.A., et al., *Use of magnetic resonance elastography to assess hepatic fibrosis in children with chronic liver disease.* J Pediatr, 2014. **164**(1), p. 186-8
24. Serai, S.D., *spin-echo echo-planar imaging Mr elastography versus gradient-echo Mr elastography for assessment of liver stiffness in children and Young adults suspected of having liver Disease.* Radiology, 2016.
25. Chang, W., *liver Fibrosis staging with Mr elastography: Comparison of Diagnostic Performance between Patients with Chronic Hepatitis B and Those with Other Etiologic Causes.* Radiology, 2016.
26. Singh, S, et al., *Magnetic resonance elastography for staging liver fibrosis in non-alcoholic fatty liver disease: a diagnostic accuracy systematic review and individual participant data pooled analysis.* Eur Radiol, 2016. **26**(5), p. 1431-40
27. Shi, Y., *Mr elastography for the assessment of hepatic Fibrosis in Patients with chronic hepatitis B infection: Does Histologic*

Necroinflammation Influence the Measurement of Hepatic Stiffness? Radiology, 2014.

28. Loomba, R., et al., *Magnetic resonance elastography predicts advanced fibrosis in patients with nonalcoholic fatty liver disease: a prospective study*. Hepatology, 2014. **60**(6), p. 1920-8

29. Yin, M., et al., *Assessment of hepatic fibrosis with magnetic resonance elastography*. Clin Gastroenterol Hepatol, 2017. **5**(10), p. 1207-1213.e2

30. DeLaPaz, R.L., *Echo-planar imaging*. Radiographics, 1994. **14**(5), p. 1045-58

31. Serai, S.D., et al., *Cross-vendor validation of liver magnetic resonance elastography*. Abdom Imaging, 2015. **40**(4). p. 789-94

32. Amatya, P., et al., *Clinical and ultrasonographic measurement of liver size in normal children*. Indian J Pediatr, 2014.0 **81**(5), p. 441-5

33. Hallgren, K.A., *Computing Inter-Rater Reliability for Observational Data: An Overview and Tutorial*. Tutor Quant Methods Psychol, 2012.**8**(1), p. 2

34. Trout, A.T., et al., *Prospective Assessment of Correlation between US Acoustic Radiation Force Impulse and MR Elastography in a Pediatric Population: Dispersion of US Shear-Wave Speed Measurement Matters*. Radiology, 2016. **281**(2), p. 544–552

35. Serai S.D, et al.,*Correlating liver stiffness with disease severity scoring system (DS3) values in Gaucher disease type 1 (GD1) patients*. Mol Genet Metab, 2018. **123**(3), p. 357-363

36. Serai, S.D., Trout, A.T., Sirlin, C.B., *Elastography to assess the stage of liver fibrosis in children: Concepts, opportunities, and challenges*. Clinical Liver Disease, 2017. **9**(1). p. 5-10

37. Serai, S.D., *spin-echo echo-planar imaging Mr elastography versus gradient-echo Mr elastography for assessment of liver stiffness in children and Young adults suspected of having liver Disease*. Radiology, 2016. **0000**, p. 10

38. Trout, A.T., et al., *Liver Stiffness Measurements with MR Elastography: Agreement and Repeatability across Imaging Systems, Field Strengths, and Pulse Sequences*. Radiology, 2016. **281**(3), p. 793-804

39. Herzka, D.A., et al., *Magnetic resonance elastography in the liver at 3 Tesla using a second harmonic approach*. Magn Reson Med, 2009. **62**(2), p. 284-91

40. Bae, J.S., et al., *Magnetic resonance elastography of healthy livers at 3.0 T: Normal liver stiffness measured by SE-EPI and GRE*. European Journal of Radiology, 2018. **107**: p. 46-53.

41. Suraj, S., *spin-echo echo-planar imaging Mr elastography versus gradient-echo Mr elastography for assessment of liver stiffness in children and Young adults suspected of having liver Disease*. Radiology, 2016.

42. Wood R Fau - Bassett, K., et al.

43. Felker, E.R., et al., *Liver MR Elastography at 3 T: Agreement Across Pulse Sequences and Effect of Liver R2* on Image Quality*. AJR Am J Roentgenol, (2018). **211**(3), p. 588-594